Article citation info:
Rezzag Bara I, Ayad ANEI, Krika W, Fezazi O, Larouci B. Magnetic pollution produced by underground XLPE 220 kV power cable in power plant. Diagnostyka. 2024;25(1):2024104. https://doi.org/10.29354/diag/177323.



DIAGNOSTYKA, 2024, Vol. 25, No. 1

e-ISSN 2449-5220
DOI: 10.29354/diag/177323

# MAGNETIC POLLUTION PRODUCED BY UNDERGROUND XLPE 220 KV POWER CABLE IN POWER PLANT

**Ilies REZZAG BARA [1], Ahmed Nour El Islam AYAD [1,*], Wafa KRIKA [2], Omar FEZAZI [3], Benyekhlef LAROUCI [1]**

[1] Department of Electrical Engineering Laboratoire de Genie Electrique, Kasdi Merbah University, Ghardaia Road, P.O. Box 511, Ouargla 30000, Algeria
[2] Department of automatic, APELEC laboratory Djilali Liabes University, Sidi Bel Abbes 22000 Algeria
[3] Department of Electrical Engineering Djillali Liabes University, Sidi Bel Abbes 22000 Algeria
[*] Corresponding author, e-mail: ayad.ahmed@univ-ouargla.dz

Abstract

The expansion of the electrical network necessitates the construction of new power plants and the extension of overhead and underground power transmission and distribution systems. However, underground power cables, such as XPLE 220 kV, can cause significant electromagnetic pollution, particularly in urban areas. This paper focuses on the evaluation and prediction of such magnetic emissions using analytical, numerical simulation (the finite element analysis), and experimental measurement. The paper aim is to minimize the magnetic emissions through the adjustment of the horizontal and vertical distances (x, y) of cables, serving as a technical solution. Additionally, the study investigated the impact of faults with varying magnitude and frequency, considering different loads and conditions. The simulation results indicate that several factors contribute to the escalation of magnetic pollution. These factors include a close proximity between cables, faults, and high current intensities.... However, as the distance between cables increases both horizontally and vertically, the strength of the magnetic field decreases, leading to a reduction in magnetic pollution. A comparison was carried out to assess the magnetic emissions of the underground cable, revealing a notable resemblance between the measured and calculated values. Ultimately, the validated simulation model serves as a valuable tool for evaluating, predicting, and mitigating electromagnetic pollution under different fault conditions and positions.

Keywords: cables, magnetic field, pollution, power, underground

## 1. INTRODUCTION

The demand for electric power in the world is increasing rapidly. Therefore, it is essential to expand the electrical network by increasing the number of power plants, substations, transformers, and extending the length of underground, overhead, and submarine transmission grids [1, 2].

However, while underground power cables are a vital component in the transportation and distribution of dynamic power flow through the electric grid. In addition, the underground power cables are characterized by simple installation and maintenance, good mechanical, thermal and electrical properties, but can generate significant magnetic emission fields in steady state [3,4 ]. Therefore, several scientific researchers have evaluated the magnetic pollution produced by overhead, submarine, and underground power transmission lines to protect human health, animals, plants, and the environment from potentially harmful impacts [4-6, 7]. For example, the electromagnetic interaction between buried gas pipelines near the electric power line are generally coupled by capacitive and inductive effects [5]. Unfortunately, the electromagnetic field can be affected by load variations and electric faults such as overload, short circuit faults, switching, and overvoltage [4-7].

The assessment of magnetic pollution is influenced by various intricate factors such as geometries, voltage levels, coupling types, and interferences in the equivalent model formulation [5]. In recent years' numerous authors have utilized analytical, semi-analytical, and numerical methods to assess the electromagnetic field due to the complex geometry of underground cables and their environment, as well as non-linear parameters such as transient states and loads. Among these methods, the Finite Element Analysis, Finite Difference Method, and Charge Simulation Method are the most commonly employed numerical techniques… [3]. Others scientific studies have investigated the interferences that occur when power transmission

Received 2023-09-12; Accepted 2023-12-19; Available online 2023-12-21

lines have higher voltage levels and are located at shorter distances in parallel position [5].

In recent times, electromagnetic interference has been observed to have adverse effects on nearby devices and connected equipment. These effects include induced current or voltage, corrosion of metallic structures, electromagnetic coupling, as well as risks to personnel safety and overall hazardous consequences [5].

Therefore, monitoring and numerically calculating several parameters of underground power cables, including electromagnetic, electric, and thermal factors, are crucial for ensuring the security and network quality and reliability [8-11].

Additionally, various techniques have been developed and applied to reduce the electromagnetic pollution caused by underground transmission lines. These techniques are classified into two types based on their magnetic induction mitigation methods:

-The passive mitigation (several conductors closed loop)

-The active mitigation, (cancel the initial magnetic induction by applying an appropriate current with the correct amplitude and phase). [4, 12, 13].

-Other simple method is proposed by changing the placement of the central phase [13].

The initial section of the paper focuses on evaluating the magnetic fields surrounding three adjacent single-core XLPE 220 kV cables [14]. The specific case under investigation serves as an example of a flat arrangement. The assessment of magnetic emissions near the cable is conducted through on-site experimental measurements, the creation of an analytical model, and the development of a mathematical model utilizing the finite element technique. mathematical model obtained will be used to simulate the magnetic field produced by three underground cables. The simulation results demonstrate the effect of various power cable conditions on magnetic pollution like: cable measurement position, rated electric current (amplitude frequencies), and limiting conditions.

This article proposes a new innovative method for reducing magnetic fields by varying the distance between the three underground phases in two axes directions (horizontal and vertical distancing) to determine the optimal depths and distances between phases. The validation of the simulation results by conducting experiments that measure magnetic flux density under different current loads was presented. The newly implemented mitigation technique aids in decreasing magnetic emissions while also minimizing the proximity effect among underground power cables through careful positioning selection.

This investigation holds great potential for integrating experiment and simulation monitoring based on magnetic emission, which can aid in detecting faults through preventive maintenance. Such an approach can improve the efficiency and clarity of the fault detection and protection process.

This paper includes a case study conducted on a power plant located at Hassi Messaoud, Ouargla, Algeria. The case study specifically focuses on a 220kV high voltage underground transmission line.

## 2. CABLE STRUCTURE PRESENTATION

Figure 1 illustrates three phases of single core 220 kV XLPE underground cable geometry and design, whosev material and shape. The conductor phase is surrounded by insulators and the conductors are additionally shielded with copper tape screens that are grounded for safety and dependable operation [14, 15].

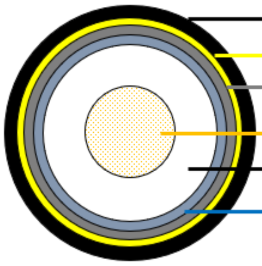


Fig. 1. High Voltage Power 220 kV XLPE underground power cable.

The Hassi Messaoud electric gas power plant, located in Ouargla, Western Algeria, uses ABB's 220 kV XLPE underground cable as a high voltage cable. The real geometrical configuration of this cable has been described in reference [14], which is used by the Sonelgaz society.

### 2.1. Materials Properties

The case study focuses on a 220 kV high voltage (three phase underground cable arranged in a flat position). Table 1 provides dimensional data, including geometry and size, for each cable domain. Table 2 presents the electric parameters of various materials, and Table 3 summarizes the electric characteristics of the underground 220 kV XLPE power cable [14, 15].

Table 1. Structure size of underground high voltage cable [14,15]

| | |
|---|---|
| Cross section (mm²) | 630 |
| conductor diameter (mm) | 29.8 |
| Insulation thickness(mm) | 23.0 |
| Diameter over insulation (mm) | 79.2 |
| Semi conductive thickness | 0.85 |
| Lead sheath thickness (mm) | 3.0 |
| Metal screen copper | 3.0 |
| Outer diameter (mm) | 112.8 |

Table 2. Materials characteristics of underground power cables [14, 15].

| Materials | Electrical conductivity $\sigma$[S/m] | Relative permittivity ($\varepsilon$) |
|---|---|---|
| Polyethylene | $1\cdot10^{-18}$ | 2.25 |
| Air | $1\cdot10^{-14}$ | 1 |
| Lead | $4.55\cdot10^{6}$ | 1 |
| Polypropylene | $1\cdot10^{-18}$ | 2.36 |
| XLPE | $1\cdot10^{-18}$ | 2.5 |
| Semi-conductive | 2 | 1 |
| Copper | $5.998\cdot10^{7}$ | 1 |
| Sand | 1 | 28 |

Table 3. Electric characteristics of XLPE cable [14, 15].

| | |
|---|---|
| Cross section | 630 $mm^2$ |
| Nominal voltage | 127/220 kV |
| Nominal current | 775 A |
| Maximum voltage | 245 kV |
| Material | copper |

## 3. MAGNETIC FIELD CALCULATION

To properly investigate the emission, distribution, and magnitude of underground magnetic cables at multiple locations, it is necessary to perform magnetic modeling and simulation. The resolution of the magnetic model can be achieved through integrative or differential equations, depending on the properties and conditions of the problem and device being studied. These equations are based on the mathematical principles described by Maxwell's equations [3, 4, 16].

Maxwell's equations comprise four partial differential equations that provide a mathematical description of how electromagnetic fields behave. These equations are based on proportional relationships that are

Combined the characteristics of materials and domains, there are what are referred to as constitutive relations. These relations encompass the set of four equations known as Maxwell's laws are [3, 16, 17]:

$$\nabla\cdot D=\rho \quad (1)$$

$$\nabla\times E=-\frac{\partial B}{\partial t} \quad (2)$$

$$\nabla\cdot B=0 \quad (3)$$

$$\nabla\times H=J \quad (4)$$

The following variables are used in this context:

$\rho$ charge density, electric induction (D), electric field (E), magnetic field (H), magnetic induction (B), and electric current density (J) [16, 18]. To establish a relation between electric field and magnetic flux density (B), the constitutive relation must be substituted:

$$B=\mu H=\mu_0\mu_r H \quad (5)$$

$$J=\sigma E \quad (6)$$

Where: $\sigma$ refers to the electrical conductivity of the conductor $\mu, \mu_0, \mu_r$ : Permeability in the medium, in a vacuum, and their relative values [16].

Based on Gauss's and current conservation laws, the relation between the electric field and the current density is represented by:

$$J=(\sigma+j\omega\varepsilon)E \quad (7)$$

Where E: electric field intensity, σ: electric conductivity, j the imaginary unit, ε refers to the permittivity and ω the angular frequency.

The current density can be describe by; $J'=J+j\omega D$ . The total current, comprising both conduction current and displacement current [6, 16]. The Maxwell-Ampere's law and the divergence of that, we obtain:

$$\nabla\times H=\nabla\times(\mu^{-1}B)=(\sigma+j\omega\varepsilon)E \quad (8)$$

We introduce the magnetic constitutive relation;

$$B=\mu H \quad (9)$$

$$(\nabla\times H)=(\nabla\times(\mu^{-1}B))=J=(\sigma+j\omega\varepsilon)E \quad (10)$$

By introduce the vector field of the magnetic vector potential A and the relation between A: the magnetic vector potential and the magnetic flux density B is written by the following equation:

$$\nabla\times A=B \quad (11)$$

Substituting equation (11) into the Maxwell-Faraday's equation: ∇× E = -jωB, the equation become:

$$\nabla\times E=\nabla\times(-j\omega A) \quad (12)$$

The relation between the magnetic vector potential and the electric field can be derived by equation

$$E=-j\omega A \quad (13)$$

Now, both B and E are represented in relation to A; if we insert this outcome into equation (14), we will find:

$$\nabla\times(\mu^{-1}\nabla\times A)=(\sigma+j\omega\varepsilon)(-j\omega A) \quad (14)$$

Finally, Substituting equation (13) and (11) into equation (10), a two Dimension partial differential equation for the magnetic vector potential A variable can be given as:

$$\nabla\times(\mu^{-1}\nabla\times A)-\omega^2\varepsilon A+j\omega A=J_s \quad (15)$$

The Finite element method (FEM) The interface employs this equation within every domain to calculate the value of A and the values of magnetic fields. [16,18].

The equations below represent the time-varying input electric current for the three phases:

$$I_a=I_0, I_b=I_0 e^{\frac{-j2\pi}{3}}, I_c=I_0 e^{\frac{j2\pi}{3}} \quad (16)$$

### 3.1. Meshing of model

The FEM model used for the study involved meshing the geometry of a 220 kV underground XLPE cable with three phases arranged in a flat configuration, as depicted in Figure (2a) [16, 18, 19]. The electromagnetic problem's boundary conditions were ensured by applying a magnetic insulation condition to the outer boundaries, represented by the following equation:

$$n \times A = 0 \tag{17}$$

a)

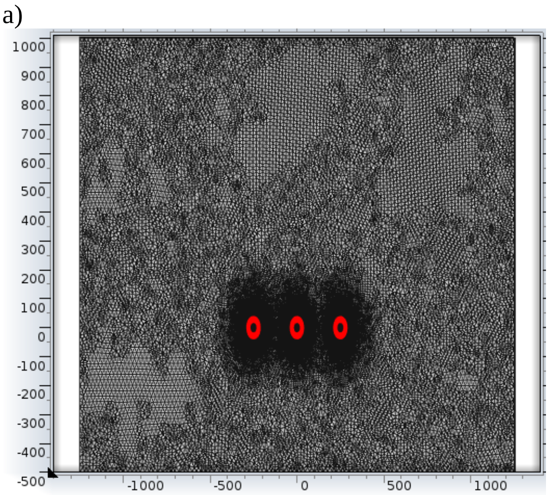

b)

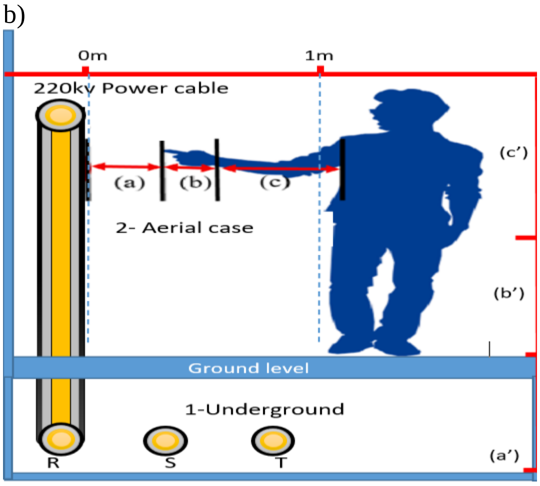


Fig. 2. Position of 220Kv underground power cable: a) meshing of the model implemented by FEM software, b) description of measurement diagram

Figure (2b) illustrates two measurement points located at distances of 0 and 1 meter from the 220kV underground power cable. These measurements were conducted in adherence to relevant regulations and safety standards, encompassing considerations such as the safe work zone, bystander proximity, and distance from other signal sources. In the first case, the power cable is positioned underground, while in the second case, it emerges from the underground channel and connects with the transformer [4].

### 3.2. Solver Configurations

When creating the underground cable model, by choosing the predefined Study (frequency, time stationary, sweep…).

- The important study steps are selection and control of equations form (physics interface od study and mesh) help to declare and edit the parameters settings before computing a solution.
- Variables and Physics (Common Study Step Settings) can be adjusted and set.

Solver Configurations consist of control nodes: one set is used to define variables for solving, while another set is dedicated to storing the solution, settings, and other relevant information.

- The solution compute give possibility to use variety of different techniques by changing and adjustments of settings.
- Adjust the preferred level of error tolerance in the solution, or determine the suitable time-integration technique and linear solver to employ.
- Extension Steps (for computation and optimization of additional settings study) [16].

## 4. SIMULATION RESULTS

### 4.1. Normal condition in Three-Core Subsea Cable

Fig. 3a shows the magnetic flux density distribution surrounding an underground XLPE 220 kV power cable placed 1 meter below the ground. The finite element method (FEM) is used to calculate the magnitude of the magnetic field around the cable's surface.

The Finite Element Method (FEM) is employed for determining the magnitude of the magnetic field in the vicinity and surface of the cable.

Simulating the underground power cable with FEM is an effective way to understand how various parameters affect the magnetic flux density.

a)

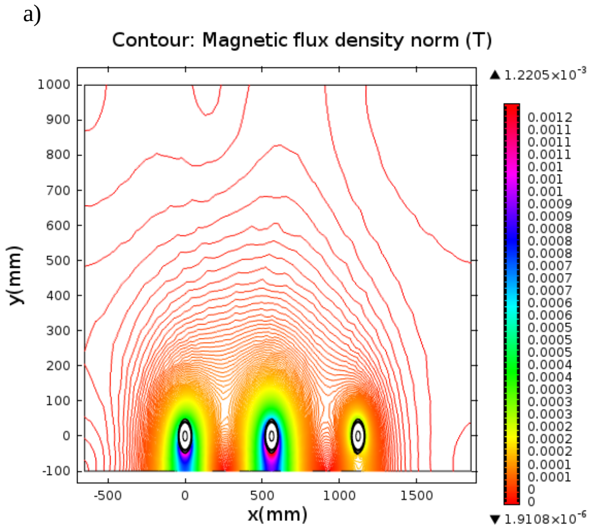

b)

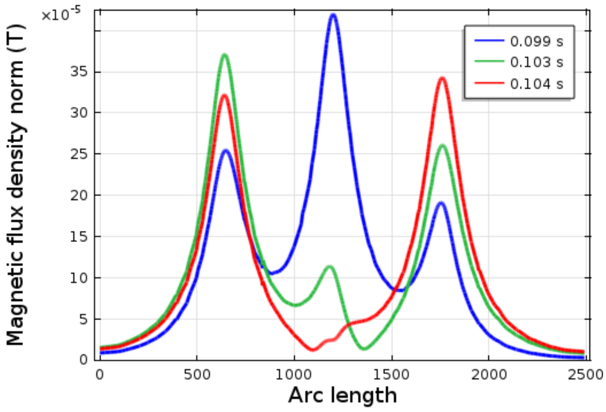


c)

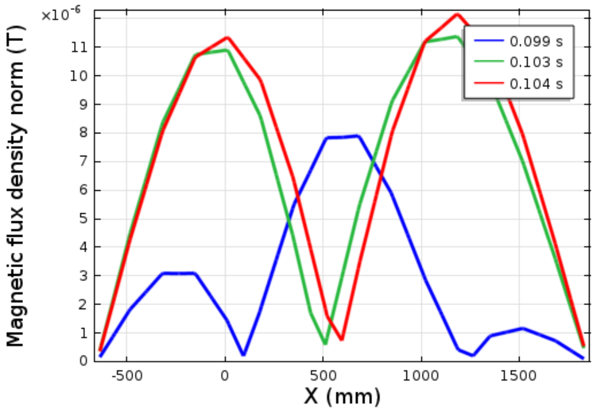


Fig. 3. Calculation of magnetic flux density: a) Magnetic field norm; b) Magnetic flux density near cable surface, c) Calculation of magnetic flux density upper 1 meter

Figure 3(b and c) displays the magnetic flux density distribution at different level above the ground surface in the vicinity of an underground cable. The cable is loaded with 720 A, and the measurements were taken at around 1 meter from the cable. From the results shown in Figure 3, one can notice that the magnetic flux density intensities and distribution are affected by both the distance and the central position of the three underground cables. It is noteworthy that the magnetic flux density values decrease as the height above the cable position and surface increases.

### 4.2. Experiment measurement:

A site test was performed on a 220 kV single-core armored XLPE underground power cable with three phases that was buried underground. This cable was located in the Hassi Massoud Ouargla gas power plant, which is part of a realistic power system network. During the test, measurements of the magnetic flux density were taken using a Teslameter device to ensure accuracy.

Teslameter characterized by three measuring ranges: 20 - 200 - 2000 mT manufactured by PHYWE for alternating and direct field with tangential hallsonde (probe) order N°:13610.93 Serial N°:220500173701 (Sensitivity: 10 µT).

The amount of current carried by a cable can vary depending on the production. This variable current affects the magnetic field generated around the power cable, specifically at the end of its sheath. In order to measure this effect, we conducted tests to measure the magnetic field outer of cable as a function of the current.

Figure 4 provides an overview of the significant measurements obtained from the cables, taking into account various factors such as current variations over a 24-hour period and magnetic field strength. The data points selected for inclusion are considered to be of particular importance. For instance, when the digital Teslameter was positioned in close proximity to the underground cable surface, a reading of 0.26 mT was recorded for a current of 236 A, as shown in Figure 4.


Fig. 4. Experimental setup of magnetic flux density measurement: 1- Teslameter, 2- probe 3-Underground power cable

Measuring electromagnetic fields can be challenging, and errors can arise from various sources for example:

1. Environmental Factors: Temperature and Humidity, Reflections and Shadows.
2. Measurement instruments and method: Frequency inaccuracies at certain frequencies response, incorrect calibration, Sensitivity, distance at different locations, Instrument Limitations.
3. Installation problems Power Supply Noise, Grounding Issues, Operator Errors, electric faults and harmonics, Transient Effects.
4. External sources of electromagnetic interference: such as radio frequency (RF) signals from communication devices, can impact measurements [20, 21].

In this paper, our aim is to assess the accuracy and reliability of a magnetic flux density model for underground power cables using FEM. To achieve this, we conducted an experimental study to monitor the electric currents and quantify the magnetic field emanating from the cable's surface.

The magnetic fields measured were then compared to simulation results, which are shown in figure 5. We calculated the error between the numerical value obtained by the FEM model and the measured value on site.

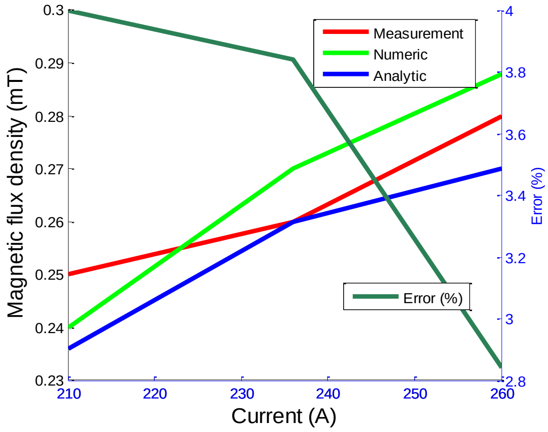


Fig. 5: Current measurement records of the XLPE 220 kV tested cable.

The analytical model can produce significant approximation errors when compared to numeric and measurement results, which can be attributed to the linear and neglected parameters of various components.

The simulation model's effectiveness was evaluated through testing with FEM and Matlab software. The model was then validated practically by conducting experiments with various current variations. The magnetic field values showed a good agreement, consistently falling within the range of measurement uncertainties. Figure5 displays the results of the comparison, indicating a strong match between the simulated and experimental values. In the case of underground cable burial, the error remained under 5%, demonstrating a very good level of accuracy [16, 22, 23].

### 4.3. Load variation

Figure 6 clearly demonstrates the relationship between magnetic flux density norm and load variation in two different positions (near and 1meter from cable). It is evident that the magnitude of magnetic flux density at various level (heights) above the underground cable surface is directly affected by the important current.

### 4.4. Distance Impact on Flat structure

#### 4.4.1. Horizontal distance variation

The effect of the distance between flat structures on the magnetic flux density is demonstrated in figure 7. This study assumes that the currents in the three phases are balanced, with varying cable locations.

The magnetic flux density magnitude of three phases is influenced by the horizontal distance, which represents the variation of their flat configuration of phases position, as shown in Fig. 7.

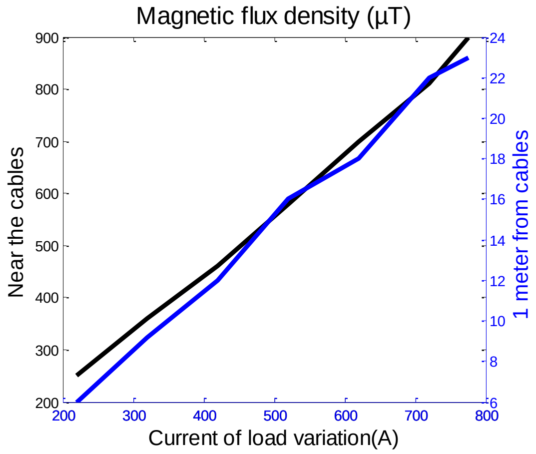


Fig .6. Load variation in underground power cables

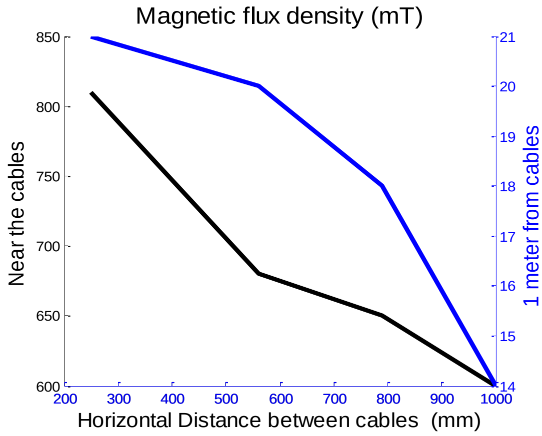


Fig. 7. Influence of horizontal distance between cables with 720 A.

According to figure 7, it is expected that the maximum magnetic field will decrease as the horizontal distance between three phases increases, which leads to the minimization of the mutual effect between the magnetic fields of the phases.

Specifically, the maximum magnetic flux density decreases from 810 μT to 600 μT when the horizontal distance is increased from 250 mm to 1000 mm.

#### 4.4.2. Vertical distance variation

Table 4 displays the effects of center, two and three phase heights on the intensity of magnetic flux density. It can be observed that the maximum flux density varies with changes in the vertical position of the phase height, (Vertical position, higher and lower than the other phases).

The magnetic flux density reached its minimum value of 12 μT when the three-phase was lowered to a height of: -125 mm in both the two-phase and three-phase cases. In contrast, the magnetic flux density was 35 μT when the phase height was: 250 mm. The magnetic field intensity values were not significantly affected by the variation in the single center phase position. This is because the significant magnetic field is generated by the other two phases, which are very near and lower than the outer phases. Varying the distance in two directions (height and horizontal) could potentially reduce and mitigate electromagnetic emissions as a classical solution.

Table 4. Influence of depth cables distance with 720 A

| | 1meter from cables Magnetic flux density (µT) | | |
|---|---|---|---|
| Vertical Distance (mm) | Center of single phase | Two phase | **Three phase** |
| -250 | 22 | 12 | 12 |
| -125 | 21 | 17 | 16 |
| 0 | 21 | 21 | 21 |
| 125 | 20 | 28 | 25 |
| 250 | 23 | 35 | 34 |

### 4.5. Abnormal conditions in underground cables (Fault)

There are four primary fault characteristics: distance, type, inception angle, and resistance. In the case of 220 kV XLPE underground power cables, three characteristics are chosen to identify single, double, and triple fault states. The faults are simulated with a 4 kA current and a frequency of 40 Hz. In the faulty phase, the current is higher compared to the healthy phase.

The presence of faults in underground cables can significantly affect the intensity and waveform of the generated magnetic field. Table 5 displays the magnetic field variations observed after introducing different fault types to the phases. When all three phases are under fault, the maximum magnetic flux density increases at various positions or levels (reaching up to 5.4 mT).

Table 5. Fault with overcurrent in three phases

| Faults Position | Single phase | Two phase | Three phase |
|---|---|---|---|
| Near cables | 0.0036 | 0.004 | 0.0054 |
| 1meter from cables | 12e-5 | 13.5 e-5 | 15 e-5 |

### 4.6. Short circuit

A short circuit can be identified by the current waveform, which exhibits varying magnitudes and frequencies depending on the type of fault, such as phase-to-phase or phase-to-ground faults. Whenever a short-circuit occurs at any point along the cable, fault signals will circulate through both the core conductor and the metal sheath. Studies suggest that in the event of a short circuit, the current for the affected phase is typically higher compared to the two healthy phases. For instance, in this paper, we propose a magnitude range of 40 kA to 90 kA at a frequency of 40 Hz for short-circuit faults.

The strength of the magnetic field amplitude is clearly dependent on the magnitude of the current fault. As shown in Table 6, the magnetic field reaches 0.16 T and 6.5 mT at near and 1 meter distances from the cable level, respectively.

Table 6. Underground under Short circuit faults

| I (kA) 20 Hz | 40 | 60 | 80 | 90 |
|---|---|---|---|---|
| B (T) Near cables | 0.068 | 0.08 | 0.14 | 0.16 |
| 1meter from cables (T) | 28e-4 | 30e-4 | 60e-4 | 65e-4 |

## 5. CONCLUSION

This paper introduces an assessment of the magnetic pollution resulting from underground power cables operating at 220 kV with three-phase XLPE insulation. The study employs a mathematical model and utilizes numeric simulations through the finite element analysis to investigate the characteristics of the underground power cable.

The simulations results show the effect of load, distance, position, frequency, and type of faults on the magnetic flux density distribution and intensities in both normal and abnormal conditions. The magnetic field intensities and distribution are computed and analyzed along a distance around the cable center at various elevations level above the ground surface. Additionally, several proposed fault conditions are simulated to show their influence on the magnetic field variation and magnitude.

The simulations involve different arrangements of the three-phase cables in both horizontal and vertical orientations. These arrangements aim to showcase the distance and width between the phases in the strongest magnetic field coupling. After applying the distancing technique solution, a comparison of the magnetic emission levels before and after reveals a significant decrease in magnetic flux density. Specifically, there is a reduction of approximately 30% in the horizontal axis and 43% in the vertical axis.

The strength of generated magnetic field can indeed affect by several parameters such as:

- Type of underground power cable component: geometries and materials characterized by different magnetic properties as lead, steel (shielding).

-The shielding help to reduce the magnetic pollution (lead or a metal jacket) , but the presence of a metal shield within the cable increase the distribution and strength of the magnetic field inside the cable and generated other problems.

Finally, through computational analysis, the effectiveness of distancing is conclusively proven as an efficient technical solution for mitigating the intensities and distribution of magnetic fields. The simulation results have been validated through a comparison with the experimental measurements, which demonstrated significant agreement.

Overall, the proposed simulation results can be used for monitoring and detection based on magnetic parameters to evaluate pollution and protect the environment. Future research will concentrate on investigating power cable failures, including experimental testing of the growth of electrical trees in underground environments, 3D simulation of subsea power cables during faults, and the assessment of magnetic pollution in the sea.

**Acknowledgment:** *The authors wish to express their gratitude to the Electric Gas Power Plant of Sonelgaz Society Company located at Hassi Messaoud Ouargla West for their invaluable assistance during the on-site experiment.*

**Source of funding:** *Our work is financed by the University of Kasdi Merbah and LAGE Laboratory of Ouargla Algeria.*

**Author contributions:** *Research concept and design, I.R.B.; Collection and/or assembly of data, A.N.I.A.; Data analysis and interpretation, W.K.; Writing the article, O.F.; Critical revision of the article, L.B.; Final approval of the article, A.N.I.A.*

**Declaration of competing interest:** *The authors declare that the article was financed from university funds and LAGE Laboratory.*

## REFERENCES

1. Krika W, Ahmed Nour El Islam A, Benyekhlef L, Benhamida F. Electromagnetic simulation of subsea power cable pollution. International Black Sea Coastline Countries Scientific Research Symposium VI Giresun, Turkey, 2021.
2. Ahmed Nour El Islam A, Krika W, Houari B, Benhamida F, Horch A. Simulation of the Electromagnetic Field in the Vicinity of the Overhead Power Transmission Line. European Journal of Electrical Engineering 2019; 21: 49–53. https://doi.org/10.18280/ejee.210108.
3. Krika W, Ayad ANE, Benyekhlef L, Benhamida F. Thermal effect of harmonic and short circuit in underground electric cable. International Black Sea Coastline Countries Scientific Research Symposium VI, Giresun, Turkey, 2021.
4. Boudjella H, Ayad ANEI, Rouibah T, Larouci B, Alghamdi TAH, Althobaiti A, i in. Magnetic field evaluation around 400 KV underground power cable under harmonics effects. Diagnostyka 2022; 23(2): 1–10. https://doi.org/10.29354/diag/150068.
5. Kurniawan A, Puspasari V, Arwati G, Khaerudini D. Investigation of AC interference on underground gas pipeline due to parallel overhead high voltage power line. 2022; 2652 s. 050017. https://doi.org/10.1063/5.0106271.
6. Krika W, Ayad ANEI, Aayad A. Magnetic field simulation of three-core submarine power cable. Acta Technica Napocensis - Series: Applied Mathematics, Mechanics, and ENGINEERING 2022; 65(2)
7. Said A, Hashima S, Fouda MM, Saad MH. Deep Learning-Based Fault Classification and Location for Underground Power Cable of Nuclear Facilities. IEEE Access 2022; 10: 70126–42. https://doi.org/10.1109/ACCESS.2022.3187026.
8. Ghoneim SSM, Ahmed M, Sabiha NA. Transient Thermal Performance of Power Cable Ascertained Using Finite Element Analysis. Processes 2021; 9(3): 438. https://doi.org/10.3390/pr9030438.
9. del-Pino-López JC, Cruz-Romero P, Bravo-Rodríguez JC. Evaluation of the power frequency magnetic field generated by three-core armored cables through 3D finite element simulations. Electric Power Systems Research 2022; 213: 108701. https://doi.org/10.1016/j.epsr.2022.108701.
10. del-Pino-López JC, Cruz-Romero P. Experimental validation of ultra-shortened 3D finite element electromagnetic modeling of three-core armored cables at power frequency. Electric Power Systems Research 2022; 203: 107665. https://doi.org/10.1016/j.epsr.2021.107665.
11. Zhu K, Han W, Lee WK, Pong PWT. On-Site Non-Invasive Current Monitoring of Multi-Core Underground Power Cables With a Magnetic-Field Sensing Platform at a Substation. IEEE Sensors Journal 2017; 17(6): 1837-1848. https://doi.org/10.1109/JSEN.2017.2651886.
12. Dein AZE, Gouda OE, Lehtonen M, Darwish MMF. Mitigation of the Electric and Magnetic Fields of 500-kV Overhead Transmission Lines. IEEE Access 2022; 10: 33900-33908. https://doi.org/10.1109/ACCESS.2022.3161932.
13. El Dein A, Gouda O, Ghoneim S, Zaini H. Mitigation of Magnetic Flux Density of Underground Power Cable and its Conductor Temperature Based on FEM. IEEE Access 2021; 1–1. https://doi.org/10.1109/ACCESS.2021.3121175.
14. Technical Catalogue and Datasheet. Underground XLPE 220 Kv Power Cable. ABB High Voltage Cables User's Guide.
15. Technical Catalogue. Maintenance Instruction and Installation Help of Underground Cable 220 kV XLPE. Electric Gas Power Plant of Sonelgaz Society at Hassi Messaoud, Ouargla, West of Algeria, The Real Geometrical Configuration.
16. Theory for the Magnetic Fields 2012. No Currents Interface User's Guide, Magnetostatic Equation AC/DC Module. Multiphysics Software COMSOL 4.3 2012. www.comsol.com/support/releasenotes/4.2/acdc.
17. Meunier G. The Finite Element Method: Theory, Implementation, and Applications. 395th edition, hardcover, Wiley 2013.
18. Karl Lonngren E, Sava Savov V, Randy Jost J. Fundamentals of Electromagnetics with MATLAB (Electromagnetic Waves). 1st and 2nd Edition, Scitech Publishing; 2nd edition (October 31, 2007).
19. Tabatabaei NM, Bizon N. Numerical Methods for Energy Applications, Springer (electronic), Power Systems, ISBN 978-3-030-62191-9. https://doi.org/10.1007/978-3-030-62191-9.
20. Govind B, Misra DK, Khanna SP, Kumar A, Bano S. Errors in Measurement of Magnetic Field and Magnetic Moment with its Associated Uncertainty. Lecture Notes in Electrical Engineering 2023; 906. https://doi.org/10.1007/978-981-19-2468-2.
21. Mathur P, Raman S. Electromagnetic Interference (EMI): Measurement and Reduction Techniques. Journal of Electronic Materials 2020; 49(5): 2975–98. https://doi.org/10.1007/s11664-020-07979-1.
22. George G, Karady E, Holbert K. Electrical Energy Conversion and Transport: An Interactive Computer-Based Approach. Chapter 5, Second Edition, John Wiley & Sons, Inc., Hoboken, New Jersey, ISBN 978-0-470-93699-3, 2013.
23. Rabah D, Djillali M. Calculation and analysis of inductive coupling effects for HV transmission lines on aerial pipelines. 2014; 90: 151–156. https://doi.org/10.12915/pe.2014.09.39.

**Ilies REZZAG BARA -** was born in El Oued, Algeria 1994. He received his master degree 2019 in electrical network from Kasdi Merbah University, Ouargla, Algeria. He is Ph.D student in Electrical engineering in Kasdi Merbah University. The interest major fields are electromagnetic pollution, electric overhead, submarine underground power cable.
e-mail: rezzagbara.ilyes@univ-ouargla.dz

**Ahmed Nour El Islam AYAD -** was born in Sidi Bel Abbes, Algeria 1985. He received his master degree in electromagnetic compatibility from Djilali LiabesUniversity, Algeria in 2011. Currently, PhD in electrotechnics from Djilali Liabes University in 2017. From 2005 to present, assistant professor in Kasdi Merbah University, Ouargla, Algeria. The major fields of research are electromagnetic pollution, eddy current and magnetic separator process.
e-mail: ayad.ahmed@univ-ouargla.dz

**Wafa KRIKA -** was born in Jijel, Algeria 1988. PHD, Professor, She is currently works in Department of automatic , Djilali Liabes , Sidi Bel Abbes 22000, Algeria . She received a Ph.D degree and Magister in Electricals engineering from the University of Science and technology of Skikda, Algeria. The interest topics are: train gear, electromagnetic pollution and separator process.
e-mail: wafa.krika@univ-sba.dz

**Omar FEZAZI -** received a master's in electromechanical engineering, Ph.D. in control of electric actuators and electrical machines from Djilali Liabes University electrical engineering faculty electrical engineering department; Algeria, in 2010 and 2017, he has been teaching at the departmentof Automatic in Djilali Liabes University electrical engineering faculty, Algeria, as an Assistant professor since 2018. Researcher at the ICEPS laboratory.
e-mail: omar.fezazi@univ-sba.dz

**Benyekhlef LAROUCI -** was born in 1985 in khelouia Mascara, Algeria. PhD Electrical Engineering, He assistant Professor at Kasdi Merbah University Ouargla, Algeria. He received a Ph.D from University of Science and technology of Oran, Algeria. His research activities are including magnetic pollution, economic dispatch, power control.
e-mail: larouci.benyekhlef@univ-ouargla.dz